Experimental Study of Operational Parameters on Product Size Distribution of Tumbling Mill

moslem mohammadi soleymani (mmsoleymani@pnu.ac.ir)
Payame Noor University

Original Article

Keywords: Tumbling Mill, Wet Grinding, Particle Size Distribution, Slurry Filling, Slurry Concentration

Posted Date: June 30th, 2020

DOI: https://doi.org/10.21203/rs.3.rs-38045/v1

Version of Record: A version of this preprint was published at Proceedings of the Institution of Mechanical Engineers, Part E: Journal of Process Mechanical Engineering on December 14th, 2021. See the published version at https://doi.org/10.1177/09544089211062763.

Experimental Study of Operational Parameters on Product Size Distribution of Tumbling Mill

M. M. Soleymani[1*]

Department of Mechanical Engineering, Payame Noor University, Bandar Abbas, Iran

Abstract:

To assess the effects of the mill operating parameters such as mill speed, ball filling, slurry concentration and slurry filling on grinding process and size distribution of mill product, it was endeavored to build a pilot model with smaller size than the mill. For this aim, a pilot mill with 1m × 0.5m was implemented. There are 15 lifters with 50mm height and face angle of 30˚. In the present work, the combination of the balls (40% of the balls with 60mm diameter, 40% of the balls with 40mm diameter and 20% of the balls with 25mm diameter) was used as grinding media with 10%, 15%, 20% and 25% of the total volume of the mill. The experiments were carried out at 60%, 70%, 80% and 90% of the critical speed. The feed of the mill is copper ore with the size smaller than 25.4 mm, which d_{80} and d_{50} of them are 12.7 and 8 mm, respectively and slurries with 40%, 50%, 60%, 70% and 80% of solid and the slurry filling between 0.5 and 2.5. The results showed that the best grinding and grading occurs at 70-80% of the critical speed and ball filling of 20-25%. Optimized grinding was observed when the slurry volume is 1-1.5 times of the ball bed voidage volume and the slurry concentration is between 60% and 70%. The mill grinding mechanism in this work is a combination of both impact and abrasion mechanisms.

Keyword: Tumbling Mill; Wet Grinding; Particle Size Distribution; Slurry Filling; Slurry Concentration.

1- Introduction

Every year, millions of tons of various metals such as copper, steel, gold, etc. produced worldwide and mills are the heart of this process. Mills are the most important part of the mining industry, as all ores enter to mineral processing plants and purification process should be firstly ground. The increase of efficiency of AG/SAG mills is the main index of energy saving. The grinding process particularly in the

* Corresponding author. Tel.: +98 76 32719974; fax: +98 76 32719974; E-mail address: mmsoleymani@pnu.ac.ir (M. M. Soleymani).

fine domain is usually the costliest part of the production of mineral processing plants and mining industries due to high energy consumption [1-2].

A number of investigators have studied the effect and the role of slurry density on the grinding behavior of ball mills [3-4]. To control slurry rheology and therefore the grinding rate, Klimpel and Austin [5-7] have employed a viscosity modifying agents. Tangsathitkulchai [8] analyzed the influence of slurry density on the breakage parameters of quartz in a laboratory ball mill. He also investigated the role of slurry density on the dynamics and behavior of wet grinding in a tumbling ball mill [9].

It is generally observed that dry and wet grinding of materials in tumbling ball mills to very fine sizes can lead to the slowing down of the overall grinding process [10-12]. Austin and Bagga [13] postulated that the slowing down of grinding rates observed in the dry systems could result from the inefficiency of particle capture by grinding media, caused by the ability of the cohesive fine particles to flow away from the ball collision zone. In this article, the mills grinding mechanism is a combination of impact and abrasion breakage mechanisms. But in previous works abrasion breakage is major mechanism in grinding.

2- Grinding Model of the Mill

For the product size distributions in a ball mill, the well-known batch grinding kinetic model proposed by Austin [10, 14] is used. The following equation represents the discrete form of the model:

$$\frac{dw_i(t)}{dt} = -S_i w_i(t) + \sum_{j=1}^{i-1} b_{ij} S_j w_j(t) \qquad , \qquad n \geq i \geq j \tag{1}$$

where t is grinding time, n is the number of size intervals, w_i is weight fraction of particles of size i, S_i is a constant termed the specific rate of breakage of size i or selection function of size i and b_{ij} is breakage function (weight fraction of particles of size i due to breakage from size j). The size distribution caused by a stone breakage from an impact is expressed via breakage function [10]. The selection function is one of the main parameters in the modeling of the ball mills. The selection function is an index of material milling process that depends on different elements such as ores properties, mill diameter, mill rotational speed, size and material of the balls [14].

In a continuum system like the mill, all materials are not subjected to the grinding at the same period, Mean Residence Time (MRT) of the particles is obtained by dividing of materials volume inside the mill (V) into the rate of flow charge (Q) as follows [1]:

$$MRT = \tau = \frac{V}{Q} \tag{2}$$

In the continuum system, some particles have a residence time less than τ, and some others have more. To determine the residence time, the value of PH is measured at the inlet and outlet of the mill at various time [1]. Fig. 1 exhibits Residence Time Distribution (RTD) in a ball mill.

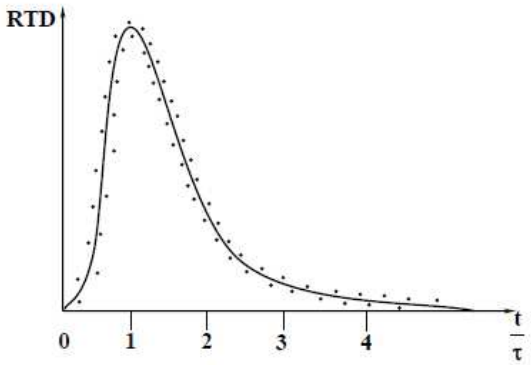

Fig. 1. Residence time distribution in a ball mill [1]

There are two main breakage mechanisms in a SAG mill: the impact breakage (high energy) and the abrasion (low energy). The JKMRC institution uses t_{10} is the percentage of breakage product that passes 1/10th of the initial particle size. Eq. 3 correlates the breakage index, t_{10}, to the specific input energy. E_{cs} is the specific breakage energy (kWh/t) as calculated from the input energy of the falling weight and the average weight of the impacted particles [15].

$$t_{10} = A(1 - e^{-bE_{cs}}) \tag{3}$$

where A is the maximum value of t_{10}, the highest level of size reduction from a single impact event, typically varying from 35% to 70% and b is the slope of the curve. It is noted that A and b are dependent parameters which they are responsible for the ore stiffness in the self-breakage mechanism. In fact, the multiplication of the aforementioned parameters is the slope of curve E_{cs}-t_{10} which is a value of ore breakage at low energy level of the SAG mill. A high value of A×b means that the rock has a low resistance to impact breakage and vice versa. The parameters of impact breakage are determined using a

high energy impact breakage apparatus which is called drop weight tester. The specific breakage energy is calculated from the following relation [15]:

$$E_{CS} = \frac{0.0272\ M_d h}{\overline{m}} \quad (4)$$

where M_d (kg) is the mass of drop weight, $\overline{m}(g)$ is the medium mass of per particle size class and h(cm) is the height of fall of drop weight. The JKMRC has defined the following equation for the abrasion breakage mechanism (t_a) [15]:

$$t_a = \frac{t_{10}}{10} \quad (5)$$

The parameter of abrasion mechanism is obtained by the test of ore abrasion exploiting a rotating experimental mill of dimensions 300mm×300mm with four lifting bars of 10mm length. It is noted that this experiment differs from the Bond work index experiment. Napier Munn et al. [15] have obtained the following equations between the impact parameters (A×b) and abrasion breakage parameters (t_a) with work index of Bond (W_i):

$$A \times b = -3.5 W_i + 117 \quad (6)$$

$$t_a = 19.7 W_i^{-1.34} \quad (7)$$

It is important to note that a few studies have been carried out for the assessment of grinding in tumbling mills and available data in this area are rather limited. However, some articles report results on the kinetic analysis and a mechanism underlying the slowing down of breakage rates in fine wet grinding in a batch laboratory ball mill [16-18] and abrasion breakage is major mechanism in that works. The numerical simulation of pulp flow investigated in the SAG mills [19], but the influences of operational parameters on the grinding of SAG mill have not been observed. In this study, the optimization of operational parameters of the SAG mill to decrease the size of final product or to increase the mill capacity regarding to downstream floatation has been carried out by an experimental pilot mill. The mill grinding mechanism in this work is a combination of both impact and abrasion mechanisms.

3- Experimental

Experimental model of the mill is illustrated in Fig. 2. In the rig, there are 15 lifters with 50mm height and face angle of 30˚. In the present work, the combination of the balls (40% of the balls with 60mm diameter, 40% of the balls with 40mm diameter and 20% of the balls with 25mm diameter) was used as grinding media with 10%, 15%, 20% and 25% of the total volume of the mill. The rotational speed of the mill motor can be adjusted continually to 100% of critical speed. The applied speeds of this study were 60%, 70%, 80% and 90% of the critical speed. In Table 1, the conditions of experiments are listed.

Fig. 2. Experimental pilot mill

Table 1. Mill characteristics and grinding conditions

Mill		
	Diameter	1000 mm
	Length	500 mm
	Speed	25, 29, 33 and 37 rpm
	Fraction of critical speed (Φ_c)	0.6, 0.7, 0.8 and 0.9
Lifters		
	Number	15
	Height	50 mm
	Face angle	30 degree
	Shape	Trapezoid, leg thickness 50 mm
Grinding media		
	Material	Chrome alloy steel
	Ball diameter	40% of the balls with 60mm, 40% of the balls with 40mm, and 20% of the balls with 25mm diameter
	Density	7800 kg/m^3
	Ball filling (J_b)	0.1, 0.15, 0.2 and 0.25 fraction of mill volume
	Total ball weight	176, 264, 352 and 440 kg
Feed		
	Material	Copper ore
	Particle size	$d_{100} = 25.4$, $d_{80} = 12.7$, $d_{50} = 8$ and $d_{10} = 0.3mm$
	Ore density	2700 kg/m^3
	Slurry concentration (C)	0.4, 0.5, 0.6, 0.7, and 0.8 (weight fraction of solid in slurry)

Slurry density	1340, 1460, 1610, 1790, and 2010 kg/m^3
Slurry filling (U)	U=0.5 - 2.5 (as volume fraction of ball bed voidage)

The feed of the mill is copper ore with the size smaller than 25.4 mm, which d_{80} and d_{50} of them are 12.7 and 8 mm, respectively. The slurry concentration used in the tests was 40%, 50%, 60%, 70% and 80%. Moreover, to investigate the influence of slurry filling (U) on the grading, the amount of slurry is increased till the slurry volume becomes 2.5 times of the balls bed voidage (the balls volume disregarding their voids). The concept of slurry filling in the mills was first introduced by Austin et al. [10]. The procedure of the experiments is such that for the investigation of four parameters; the mill speed, the ball filling, slurry concentration and slurry filling, three parameters are kept constant and the fourth parameters is varied. For each experimental condition, the mill is allowed to rotate for a set period of time, and then a specimen is taken from the product. After filter pressing, the specimens are put in the electric oven. After the cakes are dried, they are weighted. The weighted materials were then wet screened on a 325 mesh (44μm) sieve to reduce screen blinding, after which they are dried and weighted again to calculate the mass of particles smaller than 44μm. Next, the specimens are put in the shaker and screened with different sieve fractions 25400-44μm and the product particle size distribution is calculated. The sieve analysis of the product was computed based on the recorded weights of material retained on each screen and in the bottom pan.

In a pilot mill with 1m diameter, in cascading motion, the ball velocity rapidly approaches to 4m/s and it impacts at high speed in the toe region [20]. The kinetic energy of the balls with 60mm diameter and 0.88kg mass is approximately 7J. The energy of balls to grinding the copper ore feed with dimensions less than 1 inch and the average hardness is enough [21].

On experiment has been carried out to investigate whether the mill has been well designed in terms of operational parameters such as size and volume of the balls, number, height and face angle of the lifters, speed, etc or not. Therefore, 20% of the mill volume was filled with the balls. Besides, the slurry concentration is 60% and the slurry having the same volume of the balls was poured into the mill (U=1). Then, the mill worked for 10min with 75% of the critical speed.

In Fig. 3, the sizing analysis of product from the mill grinding mechanism is depicted. As seen from the figure, the mill grinding mechanism is a combination of impact and abrade breakage mechanisms. If there is just abrade mechanism, the materials remain in their initial size or a bit smaller than one, and a huge amount of small particles are produced. However, in impact mechanism, the amounts of very large and very small particles are small. Obviously from Fig. 3, there is no particle with large or medium size in the mill product while most of the particles are tiny, consequently, it can be stated that the mill grinding mechanism is a combination of both impact and abrasion mechanisms.

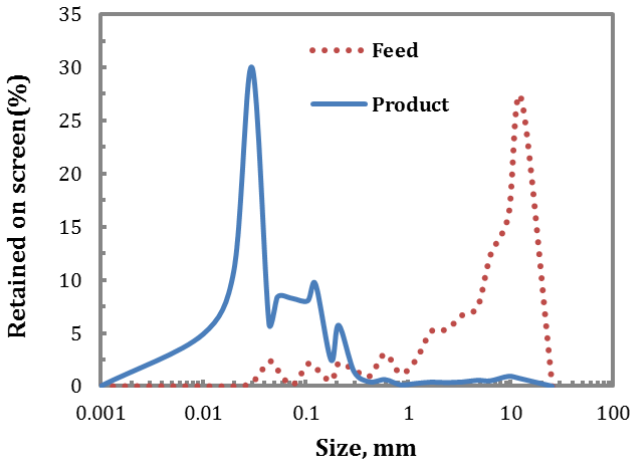

Fig. 3. Size distributions of product from the mill grinding mechanism

$(J_b = 0.2, \Phi_c = 0.75, U = 1, C = 0.6)$

The results of 27 different experiments for the assessment of the effects of the mill operational parameters such as mill speed (Φ_c), ball filling (J_b), slurry concentration (C) and slurry filling (U) on the size distributions of product are presented in the next sections. All experiments are repeated (totally 54 tests) and 2700kg of the feeding charges and 1800lit of water (totally 4.5 tons) were used in all of the tests.

4- Results and Discussion

4-1 The mill speed effects

In Fig. 4, the size distribution of the mill product has been illustrated at different speeds. To investigate the influence of speed on the grinding, the balls with 20% occupation of the mill volume (approximately 352kg) and the slurry with 60% of solid (approximately 71kg) were used. Also, the slurry volume and

volume of the balls bed voidage were the same (U=1). Table 2 shows 80% passing size, P_{80}, of the product at different speeds. Regarding to Fig. 4 and Table 2, it can be stated that the best grinding occurs at the speeds range between 70-80% of the critical speed.

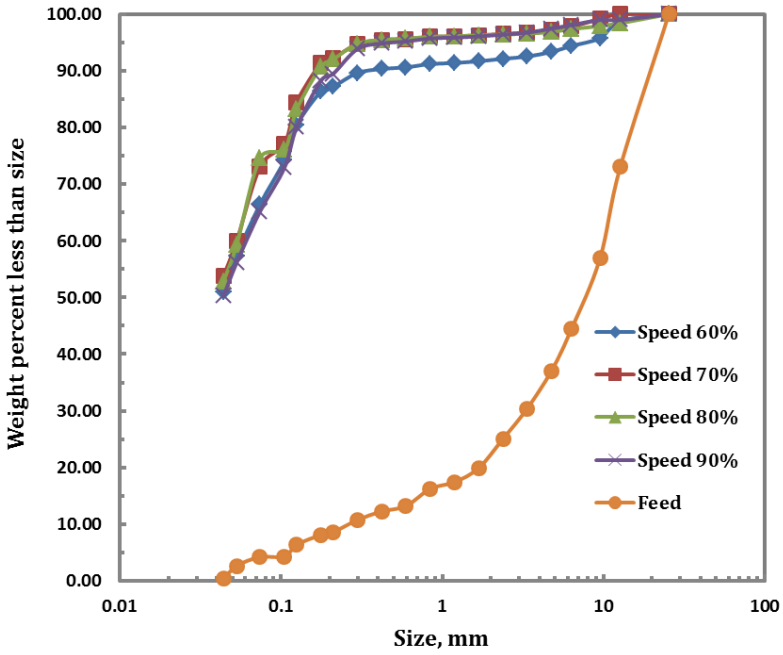

Fig. 4. Product size distributions at different mill speeds $(J_b = 0.2, U = 1, C = 0.6)$

To have better understanding of the product grinding in terms of the mill speed, the percentage of produced particles smaller than 44μm has been depicted in Fig. 5. As seen, initially with the increase of speed, the amount of particles smaller than 44μm increases, then after approaching to the peak point, the amount of such particles decreases sharply. The pick point relies at the speeds range from 70% to 80% of the critical speed depending on the slurry filling. Moreover, before the maximum point of the curve, due to the speed increase and its influence on the variation of cascade path and also due to the impact intensity, the grinding caused by the impact increases. When the mill speed increases, the shoulder of load move up, and the falling height of particles are increased in the cascading motion and as a result, the materials impact to the toe region with more speed and more energy that leads to the increase of impact grinding.

Table 2. Size distributions of product at different mill speeds
$(J_b = 0.2, U = 1, C = 0.6)$

Mill speed	Weight percent of product less than 44μm	80% passing size, P_{80}
N_c=60%	50.93%	125μm
Nc=70%	53.81%	113μm
Nc=80%	52.88%	115μm
Nc=90%	50.27%	125μm

At the speeds larger than 80% of the critical speed, the cascade path is changed due to the lifting of shoulder angle and moves toward the end of the toe. Therefore, the falling height, impact speed and impact force are lowered. Consequently, the particles and the balls have direct impact to the lifters, but due to the reduction of the speed and pressure, the grinding caused by the abrasion is lowered. Moreover, the centrifugal forces are augmented due to the speed increase. As a result, the relative velocity between the materials and the balls increase which causes the reduction of the abraded grinding rate. When the speed increases, the shoulder angle is transfered to the top and the toe angle remains almost constant. As a result, the sliding region extends and takes thin and the abraded product decreases.

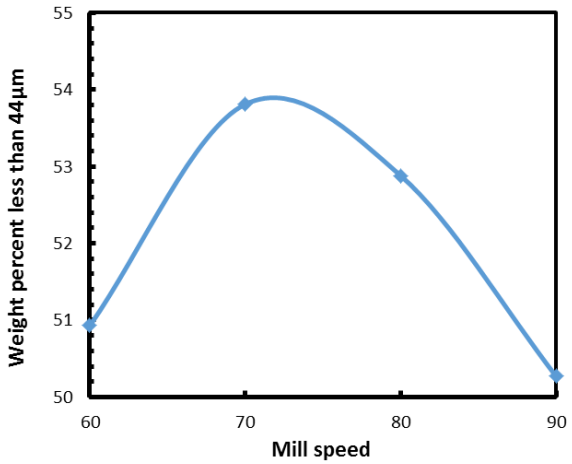

Fig. 5. Weight percent of product less than 44μm at different mill speeds

$(J_b = 0.2, U = 1, C = 0.6)$

4-2 The ball filling effects

The size distribution of the mill products under different ball filling is depicted in Fig. 6. To study the influence of the balls percentage on the grinding, the slurry with 60% solid was used while the mill speed was kept constant at 75% of the critical speed. Besides, for each experimental condition, the slurry volume and the balls bed voidage volume were the same (U=1). As observed from Fig. 6, the grinding

rate increases initially, then it decreases. Also, under 20% of the charge, the grinding rate is maximum. The rise of grinding rate is due to the increase of impacts before the peak point. It is however important that when the charge volume is small and the mill speed is high, the balls land upper than load toe and strike the lifters directly which causes the rapid failure and wear of them. Moreover, with the rise of charge and transmission of the load toe to the top, direct impact between the balls and the mill shell reduces and the balls land on the toe region, consequently, the impact grinding increases. Furthermore, after the peak point, the grinding rate reduces with the increase of ball filling. With the increase of ball charge, the shoulder angle remains almost constant while the toe height increases, thus, the balls have short falling height and in turn the grinding due to the impact is reduced. In addition, with the increase of the load weight and the increase of pressure on the sliding region, the displacement and slide of the materials are lowered and thus the grinding rate due to abrasion is decreased.

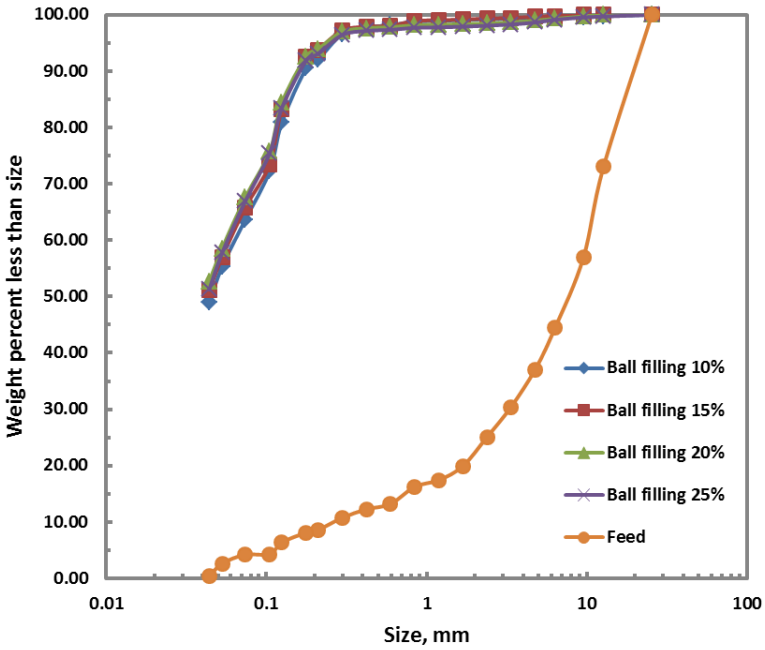

Fig. 6. Size distributions of product at different ball filling $(\Phi_c = 0.75, U = 1, C = 0.6)$

Addition of the balls charge from 10% to 25% requires that the powder charge should rise to keep the value of U constant. Thus, the slurry weight should be increased from 35kg to 89kg. As the slurry volume increases, by assuming that the rate of flow charge of the mill remains constant, the residence time of the materials in the mill rises ($\tau = V/Q$). To examine the influence of residence time in this test, the

experiment were repeated for different balls charges, however, in each test, the residence time was different with respect to slurry volume. At 10% of the balls charge and the slurry weight of 35kg, the residence time became 7.5min. Also, this time for the other charges were 11.25, 15 and 18.75min, respectively. In Table 3, 80% passing size, P_{80}, and in Fig. 7 the percentage of produced particles smaller than 44μm for two cases of similar and variable residence time are presented which demonstrate that the grinding is optimum at charges between 20% and 25%.

Table 3. Size distributions of product at different ball filling $(\Phi_c = 0.75, U = 1, C = 0.6)$

Ball filling	Ball weight	Slurry weight	Similar residence time			Variable residence time		
			MRT	Weight percent less than 44μm	80% passing size, P_{80}	MRT	Weight percent less than 44μm	80% passing size, P_{80}
$J_b = 10\ \%$	176kg	35kg	$\tau = 15$ min	48.91%	123μm	$\tau = 7.5$ min	41.56%	150μm
$J_b = 15\ \%$	264kg	53kg	$\tau = 15$ min	51.09%	119μm	$\tau = 11.25$ min	47.57%	132μm
$J_b = 20\ \%$	352kg	71kg	$\tau = 15$ min	52.59%	115μm	$\tau = 15$ min	52.59%	115μm
$J_b = 25\ \%$	440kg	89kg	$\tau = 15$ min	51.22%	117μm	$\tau = 18.75$ min	52.51%	115μm

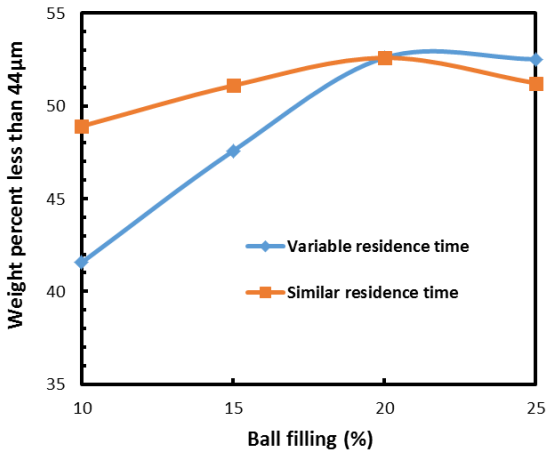

Fig. 7. Weight percent of product less than 44μm at different ball filling $(\Phi_c = 0.75, U = 1, C = 0.6)$

4-3 The slurry filling effects

To examine, the influence of U on the grinding, the mill speed was set to 75% of the critical speed and the slurry with 60% of solid was used. Besides, the balls filled 20% of the mill volume (almost 352kg). In Fig. 8, the variation of grinding in terms of slurry filling was depicted. Apparently from Fig. 8, the best grinding occurs at U=0.5, in which with the increase of slurry volume and the pool formation, the grinding decreases. It is noted that with the increase of slurry volume, the pool is formed in the mill for

U≥1, consequently, the impact loads is absorbed and damped by the pool. Also, with the decrease of impact loads, the contribution of grinding due to the impact is lowered and with the constancy of grinding due to the abrasion, the total grinding is reduced. It is important however to state that on the one hand, with the increase of slurry volume and the increase of materials weight in the mill, the normal force on the materials should be increases, but on the other hand, with the formation of pool, the buoyancy (Archimedes) force on the materials is increased in which the resultant normal force is lowered. Therefore, the normal force effects can be ignored.

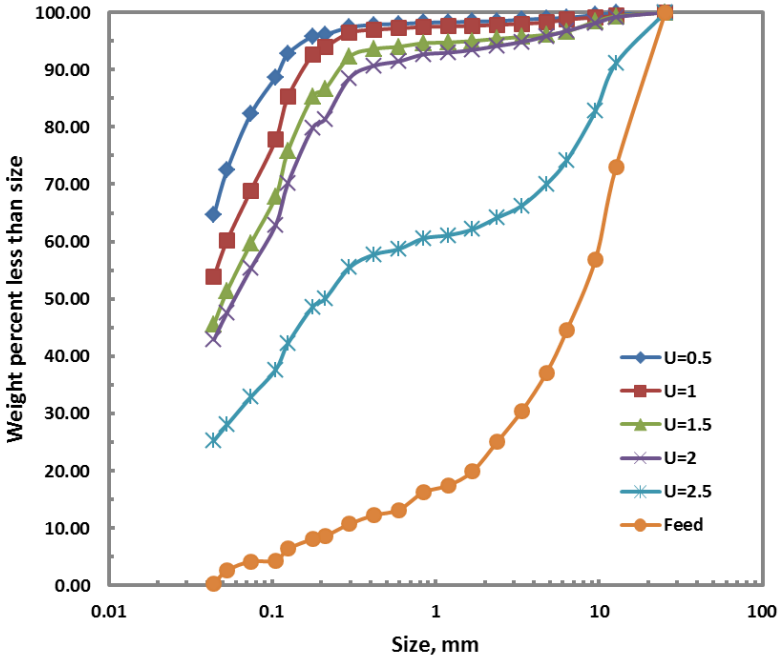

Fig. 8. Size distributions of product at different slurry filling for similar residence time ($\Phi_c = 0.75, J_b = 0.2, C = 0.6$)

Moreover, with the increase of slurry volume, when the rate of flow charge is kept constant, the residence time increases. The tests associated to Fig. 8 are presented in Fig. 9 for different values of the residence time. The residence time was chosen to be 5min and 10min for U=0.5 and 1, respectively. In Fig. 10, the percentage of the produced particles smaller than 44μm is shown in terms of the slurry volume under various residence times and under the same residence time. According to Fig. 10 and Table 4, the best grinding occurs at the slurry filling between 1 and 1.5. Also, if the residence time is similar, with the increase of U, the size distribution of product becomes larger. Instead, if the residence time is not

similar, initially with the increase of U, the grinding is improved in which its maximum occurs at U=1.5, after that, the grinding is lowered again.

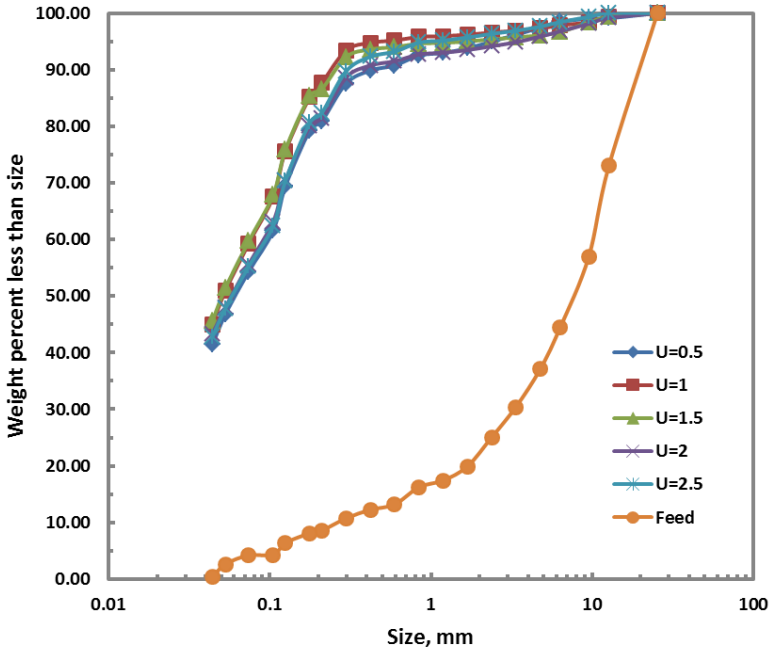

Fig. 9. Size distributions of product at different slurry filling for variable residence time ($\Phi_c = 0.75, J_b = 0.2, C = 0.6$)

Table 4. Size distributions of product at different slurry filling ($\Phi_c = 0.75, J_b = 0.2, C = 0.6$)

Slurry filling	Ball weight	Slurry weight	Similar residence time			Variable residence time		
			MRT	Weight percent less than 44μm	80% passing size, P_{80}	MRT	Weight percent less than 44μm	80% passing size, P_{80}
$U = 0.50$	352kg	35kg	$\tau = 15$ min	64.67%	70μm	$\tau = 5$ min	41.39%	190μm
$U = 1.00$	352kg	71kg	$\tau = 15$ min	53.89%	110μm	$\tau = 10$ min	45.02%	150μm
$U = 1.50$	352kg	106kg	$\tau = 15$ min	45.56%	150μm	$\tau = 15$ min	45.56%	150μm
$U = 2.00$	352kg	142kg	$\tau = 15$ min	42.88%	180μm	$\tau = 20$ min	43.30%	175μm
$U = 2.50$	352kg	177kg	$\tau = 15$ min	25.29%	8500μm	$\tau = 25$ min	42.76%	177μm

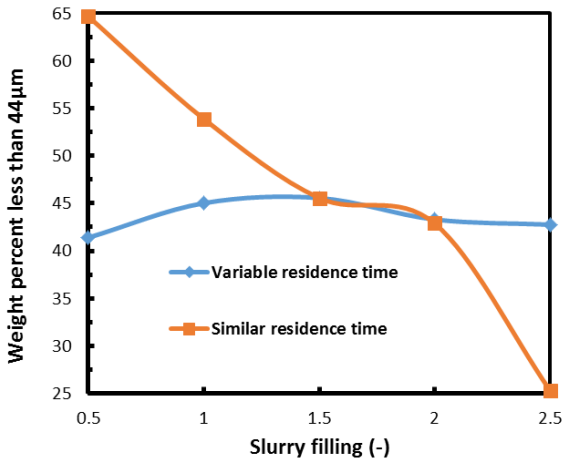

Fig. 10. Weight percent of product less than 44µm at different slurry filling ($\Phi_c = 0.75, J_b = 0.2, C = 0.6$)

Furthermore, the formed slurry pool in the mill has profound effect on the absorption of the balls energy [22, 23]. In other words, with the formation of slurry pool, the energy due to the impact loads is lowered and the contribution of impact to the grinding is reduced. Fig. 11 exhibits that with the increase of U from 0.5 to 1.5 and then to 2.5, the values of impact forces reduce. These impact forces were measured using a load cell mounted under one of the lifters for one rotation of the mill. It is noted that the coordinate was chosen to be at 12:00 o'clock and all angles were measured based on that point. According to Fig. 11, with the increase of formed pool level and also with the increase of slurry density, the pool acts like a damper at which the impact loads decrease more and consequently the grinding due to the impact is lowered.

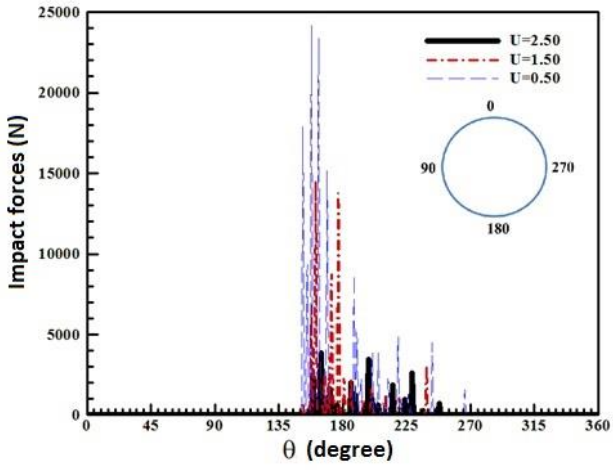

Fig. 11. Impact forces in one rotation of the mill at different slurry filling ($\Phi_c = 0.75, J_b = 0.2, C = 0.6$)

4-4 The slurry concentration effects

The particle size distribution of the products at different density of slurry (or slurry concentration) was depicted in Fig. 12. In order to assess the influence of density on the grinding, the mill is allowed to rotate with 75% of the critical speed and the balls with the weight of 352kg have occupied 20% of the mill volume. Also, the slurry with 40-80% of the solid as a feed charge with approximate weight of 59-88kg was used. In each tests, the slurry filling was chosen to be unity. In Table 5, 80% passing size, P_{80}, has been shown under various concentrations. Comparison between the results obtained from different densities reveals that the grinding rate is more at low concentration due to the low viscosity and density of the slurry and consequently the increase of relative speed between the balls and the materials. According to Fig.12 and Table 5, it is clear that the grinding is maximum for the slurry with 40% of solid compared to the other concentrations. It is because of the fact that whatever the slurry density and viscosity are low, the particles move more simply among the balls and cross the liners with higher speed, therefore, the abrasion grinding improves. At the concentration of 40%, 352 kg of the balls should grind 59kg of the slurry while this amount of the balls at the concentration of 50% should grind 64 kg of the slurry. Therefore, the possibility of the balls impact to the mill materials is higher at the concentration of 40%, so better grading is obtained. It is noted that the same amount of the balls should grind 71, 79 and 88 kg of the slurry at the concentration of 60%, 70% and 80%, respectively.

In addition, if the percentage of slurry solid is low, it causes formation of a pool in the mill, the contact between metal to metal, the increase of the balls consumption and the escape of the material among the balls. Also, a large volume of the mill is filled with water which practically reduces the mill efficiency. Besides, in the next stages, the drying process is costly. On the other hand, at very high density and viscosity, the slurry acts as a damper and creates resistance of the balls movements against impact. Consequently, the impact grinding speed improves with the reduction of slurry viscosity. So, the best viscosity for the minimum abrasion time is for slurry with 60-70% of the solid.

From Fig. 13, the percentage of produced materials smaller than 44μm for concentration of 40%, 50%, 60% and 70% are 55.68%, 52.68%, 51.05% and 47.85%, respectively. However, the best grinding is obtained at 40% of concentration, but it is noted that for a condition that the mill speed, the balls volume, the slurry filling and the residence time are similar, at concentration of 70%, 34% more solid feed can be

ground compared to concentration of 40% (79/59=1.34). This ratio is 8% and 20% more than the concentration of 40% for the concentration of 50% and 60%, respectively. In the other word, P_{80} at the concentration of 40% is 80μm and at the concentration of 70% is 130μm. But, the rate of feed flow in the slurry of 70% is almost 34% more than the slurry of 40%.

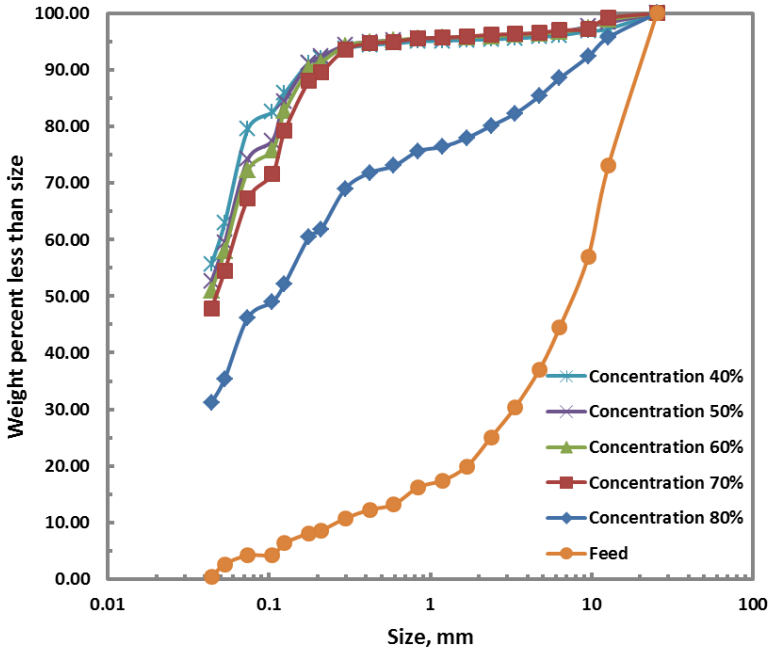

Fig. 12. Size distributions of product at different concentration

($\Phi_c = 0.75, J_b = 0.2, U = 1$)

Table 5. Size distributions of product at different concentration

($\Phi_c = 0.75, J_b = 0.2, U = 1$)

Slurry concentration	Slurry weight	Weight percent less than 44μm	80% passing size, P_{80}
$SC = 40\%$	59kg	55.68%	80μm
$SC = 50\%$	64kg	52.68%	112μm
$SC = 60\%$	71kg	51.05%	117μm
$SC = 70\%$	79kg	47.85%	130μm
$SC = 80\%$	88kg	31.15%	2350μm

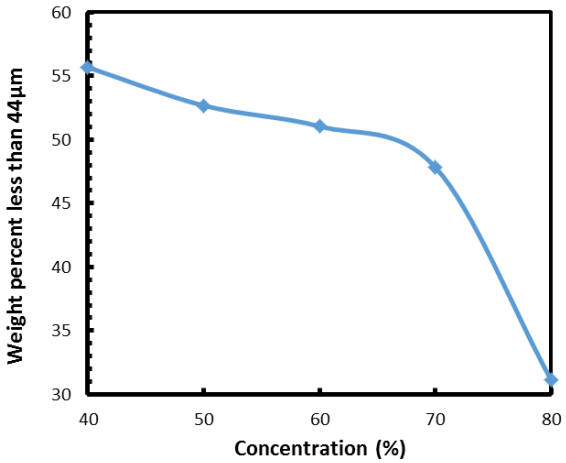

Fig. 13. Weight percent of product less than 44µm at different concentration ($\Phi_c = 0.75, J_b = 0.2, U = 1$)

With the formation of slurry pool and the increase of its density, the energy of impact forces reduces and thus, the contribution of impact in grinding is lowered. With the increase of slurry concentration from 40% to 60% and then to 80%, the values of impact forces are reduced according to Fig. 14. The materials packing between lifters and the walls at the concentration of 80% are plotted in Fig. 15. The packing is due to the fact that the grading of slurry of 80% is quite different than the other results.

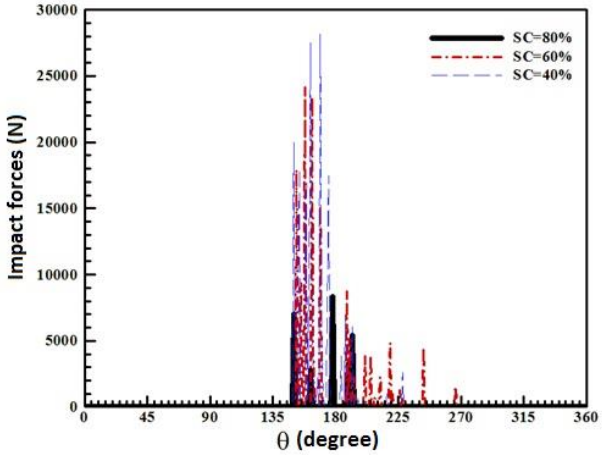

Fig. 14. Impact forces in one rotation of the mill at different concentration ($\Phi_c = 0.75, J_b = 0.2, U = 1$)

Fig. 15. The materials packing between lifters and the walls at the concentration of 80%

5- Conclusions

The present paper aimed to study the effect of mill speed, ball filling, slurry filling and slurry concentration on the particle size distribution of product in the SAG mills. The pilot mill (1000×500 mm), initially loaded with balls at four different charges from 10% to 25% volumetric filling, was run at four different speeds varied from 60% to 90% of the critical speed. The tests covered a range of slurry filling (U) from 0.5 to 2.5 using of a feed of -1 inch copper ore with 40% to 80% slurry concentration. The following conclusions can be drawn from the present work:

- The best grinding and grading occurs at 70-80% of the critical speed. The grinding decreased before and after of this range.
- Under 20-25% of the ball filling, the grinding rate is maximum.
- Optimized grinding is observed when the slurry volume is 1-1.5 times of the ball bed voidage volume.
- The best grinding and grading occurs at the slurry concentration between 60% and 70%. The materials' packing between lifters and the walls is at the concentration of 80%.
- With the increase of slurry volume, the pool is formed in the mill, with the increase of formed pool level and also with the increase of slurry concentration and density, the pool acts like a damper at which the impact loads decrease more and consequently the grinding is lowered.

Availability of data and materials

Not applicable

Competing interests

Not applicable

Funding

Not applicable

Authors' contributions

Not applicable

Acknowledgments

The present work was financially supported by the NICICO. Special thanks to the generous helps of R&D and the concentrate unit of the NICICO.

References

1. King, R.P., 2001, modeling and simulation of mineral processing systems, Elsevier.
2. Bond, F.C., 1961, crushing and grinding calculations, Allis-Chalmers Manufacturiing Company.
3. Tangsathitkulchai, C., Austin, L.G., 1985, The effect of slurry density on breakage parameters of quartz, coal and copper ore in a laboratory ball mill, Powder Technology, 42, 287– 296.
4. Tangsathitkulchai, C., Austin, L.G., 1989, Slurry density effects on ball milling in a laboratory ball mill, Powder Technology, 285– 293.
5. Klimpel, R.C., Austin, L.G., 1982, Chemical additives for wet grinding of minerals, Powder Technology, 31, 2, 239-253.
6. Klimpel, R.C., Austin, L.G., 1983, A preliminary model of liberation from a binary system, Powder Technology, 34, 1, 121-130.
7. Austin, L.G., Klimpel, R.C., 1985, A note on the prediction of specific rates of breakage for an equilibrium ball charge, Powder Technology, 43, 2, 199-201.
8. Tangsathitkulchai, C., 2002, Acceleration of particle breakage rates in wet batch ball milling, Powder Technology, 124, 67–75.
9. Tangsathitkulchai, C., 2003, The effect of slurry rheology on fine grinding in a laboratory ball mill, International Journal of Mineral Processing, 69, 29-47.
10. Austin, L.G., Klimpel, R.R., Luckie, P.T., 1984, the Process Engineering of Size Reduction: Ball Milling. SMEAIME, New York, pp. 99– 110.
11. Frances, C., Laguerie, C., 1998, Fine wet grinding of an alumina hydrate in a ball mill, Powder Technology, 147–153.
12. Yekeler, M., Ozkan, A., Austin, L.G., 2001, Kinetics of fine wet grinding in a laboratory ball mill, Powder Technology, 114, 224– 228.
13. Austin, L.G., Bagga, P., 1981, An analysis of fine dry grinding in ball mills, Powder Technology, 28, 83– 90.

14. Austin, L.G., 1999, A discussion of equations for the analysis of batch grinding data, Powder Technology, 106, 71–77.
15. Napier–Munn, T.J., Morrel, S., Morrison, R. D. and Kojovic, T., 1996, Mineral comminution circuits, JKMRC, Australia, 318-320, 332.
16. Austin, L.G., Shah, I., 1983, A method for inter-conversion of Microtrac and sieve size distributions, Powder Technology, 35, 271–278.
17. François K.M., Moys, M.H., 2014, Effects of slurry pool volume on milling efficiency, Powder Technology, 256, 428-435.
18. Moys, M.H., 2015, Grinding to nano-sizes: Effect of media size and slurry viscosity, Minerals Engineering, 74, 64-67.
19. Cleary, P.W, Morrison, R.D., 2012, Prediction of 3D slurry flow within the grinding chamber and discharge from a pilot scale SAG mill, Minerals Engineering, 39, 184–195.
20. Rezaeizadeh, M., Fooladi, M., Powell, M.S., Mansouri, S.H., Weerasekara, N.S., 2010, A new predictive model of lifter bar wear in mills, Minerals Engineering, 23, 15, 1174-1181.
21. Tavares, L.M., 2007, Breakage of single particles: quasi-static. In: Salman, A.D., Ghadiri, M., Hounslow, M.J. (Eds.), Handbook of Particle Breakage, vol. 12, Elsevier, 3–68.
22. Soleymani, M.M., Fooladi, M. and Rezaeizadeh, M., 2016. Effect of slurry pool formation on the load orientation, power draw, and impact force in tumbling mills. Powder Technology, 287, pp.160-168.
23. Soleymani, M.M., Fooladi Mahani, M. and Rezaeizadeh, M., 2017. Experimental study the impact forces of tumbling mills. Proceedings of the Institution of Mechanical Engineers, Part E: Journal of Process Mechanical Engineering, 231(2), pp.283-293.

Figures

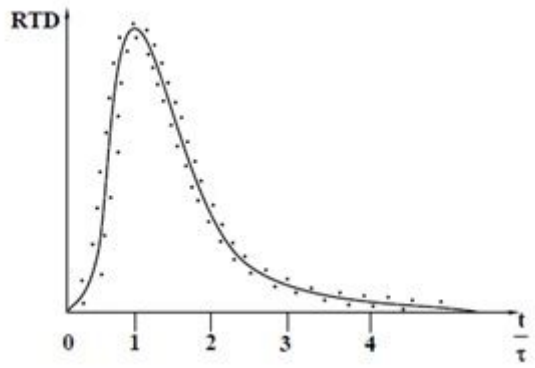

Figure 1

Residence time distribution in a ball mill [1]

Figure 2

Experimental pilot mill

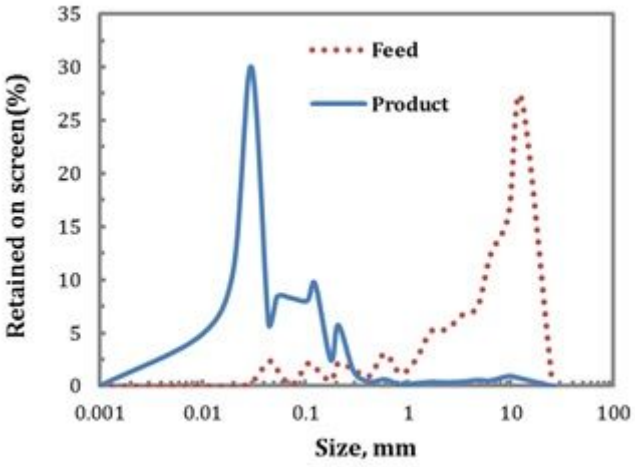

Figure 3

Size distributions of product from the mill grinding mechanism (Jb=0.2, Φc=0.75, U = 1, C=0.6)

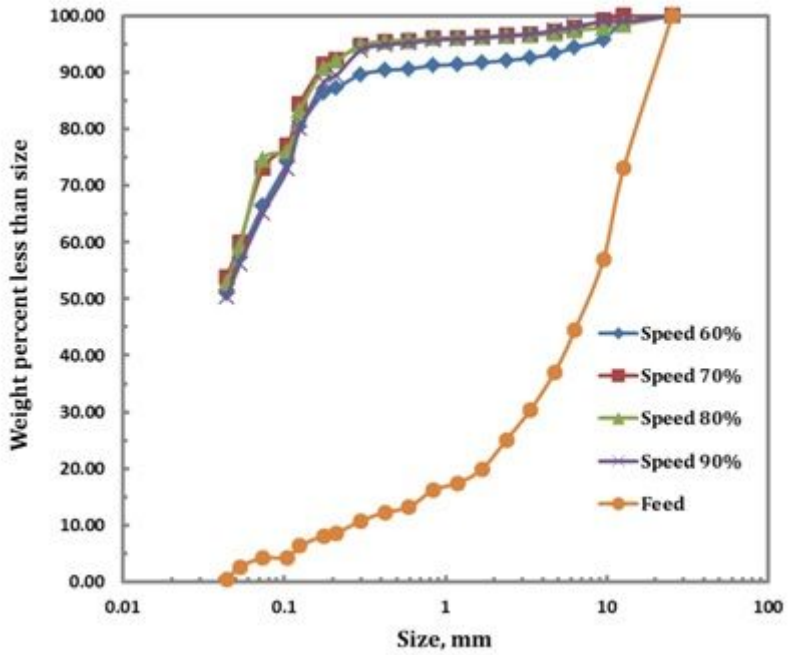

Figure 4

Product size distributions at different mill speeds (Jb = 0.2, U = 1, C = 0.6)

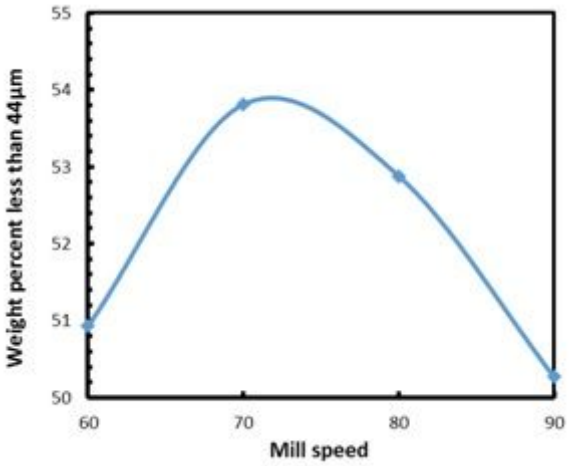

Figure 5

Weight percent of product less than 44µmat different mill speeds (Jb = 0.2, U = 1, C = 0.6)

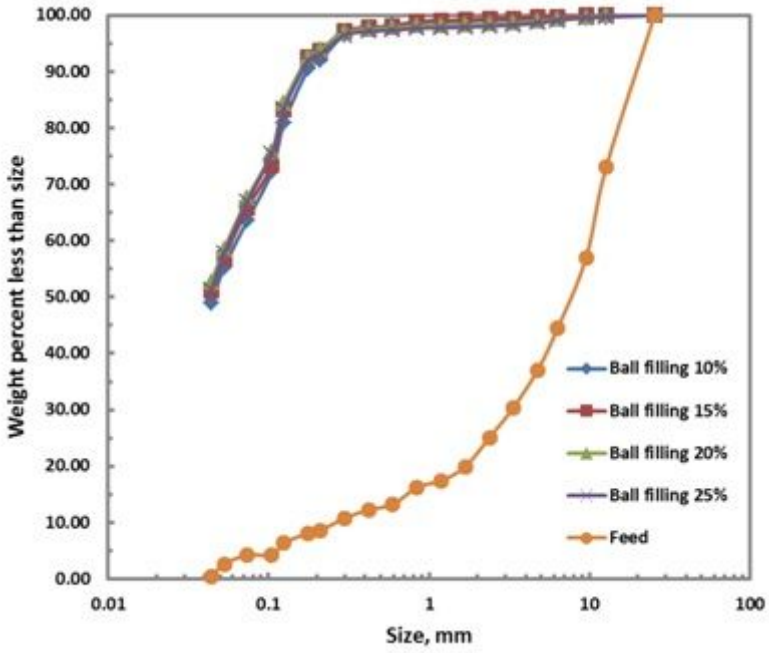

Figure 6

Size distributions of product at different ball filling (Φc=0.75, U=1,C=0.6)

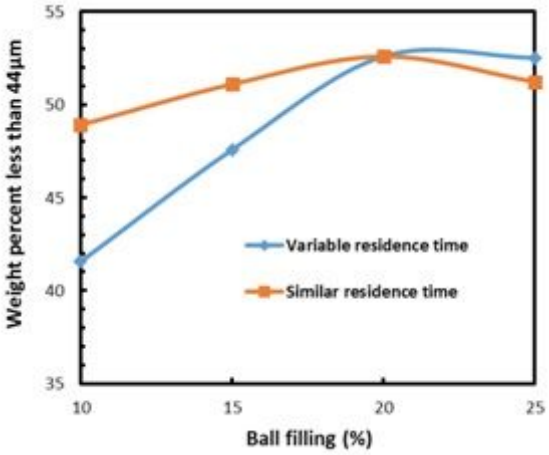

Figure 7

Weight percent of product less than 44μm at different ball filling (Φc=0.75, U=1,C=0.6)

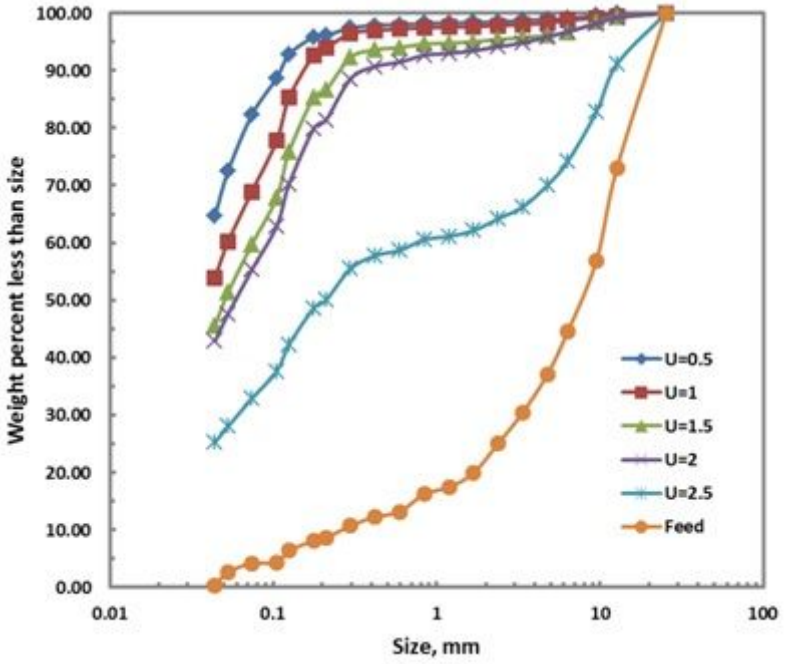

Figure 8

Size distributions of product at different slurry filling for similar residence time (Φc=0.75, Jb=0.2, C=0.6)

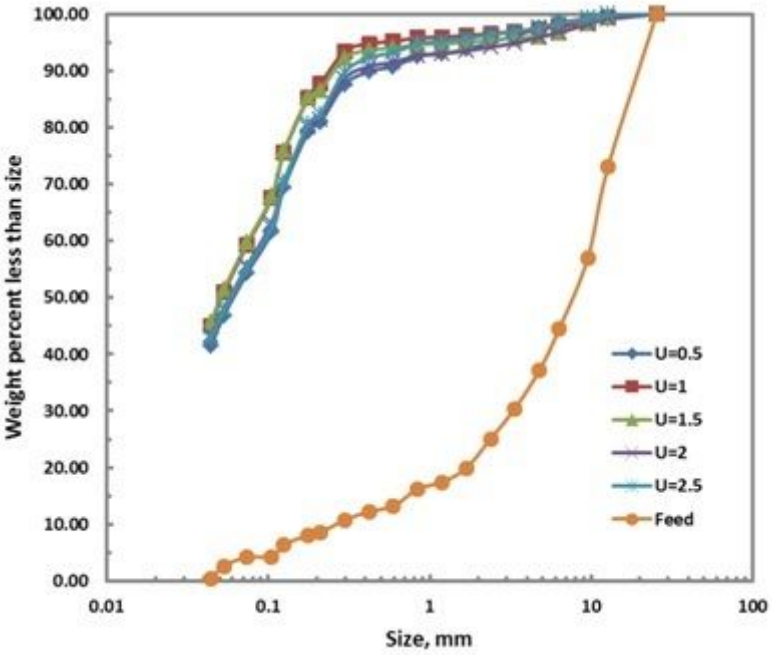

Figure 9

Size distributions of product at different slurry filling for variable residence time (Φc=0.75, Jb=0.2, C=0.6)

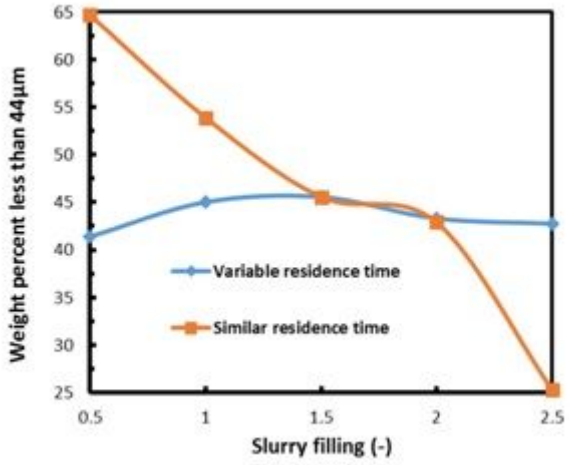

Figure 10

Weight percent of product less than 44μm at different slurry filling (Φc=0.75, Jb=0.2, C=0.6)

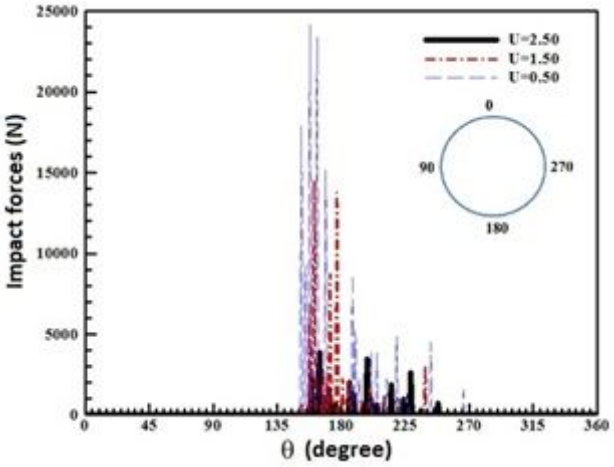

Figure 11

Impact forces in one rotation of the mill at different slurry filling (Φc=0.75, Jb=0.2, C=0.6)

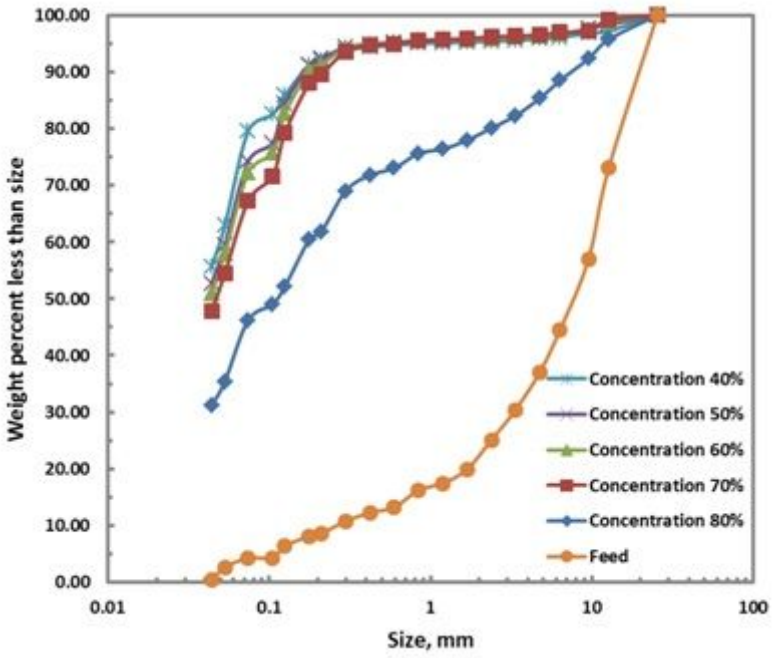

Figure 12

Size distributions of product at different concentration (Φc=0.75, Jb=0.2, U=1)

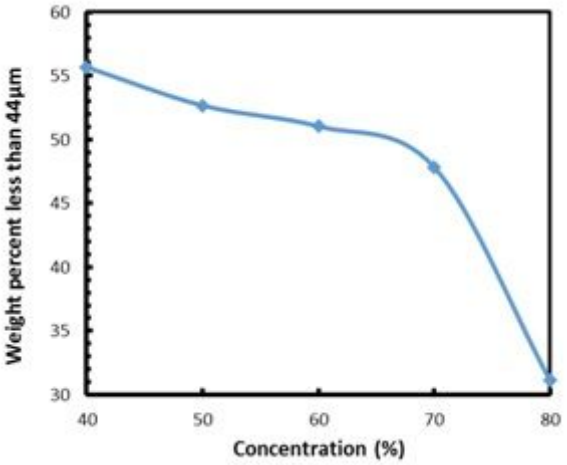

Figure 13

Weight percent of product less than 44µm at different concentration (Φc=0.75, Jb=0.2, U=1)

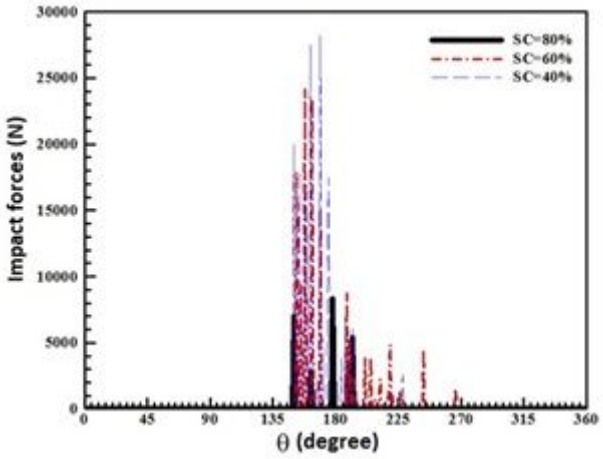

Figure 14

Impact forces in one rotation of the mill at different concentration (Φc=0.75, Jb=0.2, U=1)

Figure 15

The materials packing between lifters and the walls at the concentration of 80%